Dynamic Modelling of Wind-Solar-Storage Based Hybrid Power Plant

Kaushik Das, Anca D Hansen, Panagiota Adamou,
Xenofon Giagkou, Filippos Rigas
Jayachandra Sakamuri and Poul E Sørensen
Technical University of Denmark
Email: kdas@dtu.dk

Müfit Altin
Energy Systems Engineering Department
Izmir Institute of Technology
Turkey

Edgar Nuño
Suzlon Energy Limited
Germany

***Abstract*—This paper presents the modelling and the control architecture of two different hybrid power plant topologies, e.g. AC and DC coupled Wind-Solar-Storage based Hybrid Power Plants. Dynamic models of different individual assets are briefly described in the paper. A set of simulations are carried out in order to verify and demonstrate the performance of the dynamic models and of the hybrid power plant control dispatch strategy for different control functionalities - namely, maximum power point tracking, delta control and balance control. An overview of the modelling challenges and complexities of ancillary services provisions from hybrid power plants is provided and discussed.**

I. Introduction

Increasing awareness for climate change and fossil free electricity generation in future is driving the energy systems globally to install more and more wind and solar power generations. This is further accelerated with fast reducing costs of variable renewable energy (VRE) sources like wind turbines (WT) and solar photovoltaics (PV) technology. However, to accommodate these fast development the power system infrastructure needs to be reinforced. To allow fast growth of VRE integration without being limited by grid reinforcement, one option could be to combine wind and solar generation to optimally utilize the grid resources. Combination of wind and solar is also logical since wind and solar resources are very loosely correlated if not negatively correlated [1]. At the same time, reduction of levelized cost of energy for onshore wind farms is reaching the minimum value. Power curtailment previously an unthinkable economic burden for renewables looks viable scenario in the future power systems with large share of renewables in power grids. At the same time, prices for solar photovoltaics and storage are sharply reducing [2].

These benefits among others [1] have increased the focus on development of utility scale wind-PV-storage based hybrid power plants (HPPs) all over the world. Very recently, WindEurope has come up with a position paper on HPP listing all the HPP projects [3]. Windlab and Vestas have installed the first utility scale wind-solar-battery Kennedy Energy Park Hybrid power plant in 2018. There are only 3 HPPs with capacity more than 50 MW namely, Vattenfalls 64 MW Haringvliet, The Netherlands; 78.8 MW Kavithal project, India; 60 MW Kennedy Energy Park, Australia. India has come out with National Wind-Solar Hybrid Policy and intends to launch 2.5 GW auction.

One of the major advantages of combining wind and solar power generation is optimal utilization of electrical infrastructure inside the HPP. For example, either connecting the resources at AC connection point or connecting different resources at the DC bus of the wind turbine, can be different options to connect the generation sources. However, different types of configurations have different control complexities and control architecture [4], [5]. For example, an AC connected wind farm, solar farm and battery energy storage system (BESS) comprising HPP has a wind park controller, solar park controller and BESS controller. However, an HPP controller acts as supervisory control to send different dispatch signals to individual controllers. Whereas, in an HPP where solar panels and Battery storage are connected to the DC bus of the wind turbine through DC-DC converters, the control architecture is quite different. In such an architecture, there may be no specific advantage to have separate wind park controller, solar park controller and BESS controller, rather a single HPP controller can be sufficient.

Dynamic models of all these different configurations need to be developed in order to perform dynamic studies such as for ancillary services provision, power system stability support etc. It should be noted that the dynamic models also differ for different purpose of studies, namely, active power support, reactive power support, fault ride through, frequency support etc.

This paper discusses different dynamic models and control hierarchies for AC and DC connected HPP configurations. The performances of these dynamic models are simulated for different control functions, namely - maximum power point tracking control, balance control and delta control. Modelling complexities and challenges for ancillary service provision from HPP are also discussed briefly.

II. Hybrid Power Plant Topologies

Different HPPs topologies are described in details in [2] in order to distinguish the generic infrastructure of HPPs. In this section the focus will be laid on the AC-coupled and DC-coupled HPP solutions, as shown in Fig. 1 and Fig. 2 respectively.

As depicted in Fig. 1, in the AC-coupled HPP solution, the assets have individual points of connection being connected to the external grid through the same transformer. The WT's connection involves a full-scale back-to-back converter, while the PVs are connected through both a DC-DC converter, that increases the panels output voltage level, and an inverter. The BESS's connection requires only an inverter.

The main advantage of the AC-coupled HPP topology is that it is easily expandable since more systems can be added in parallel to either increase the storage power or the overall HPP capacity [6]. Another major advantage is the usage of Wind power plant (WPP) controller, PV controller and BESS controller in its current form, which makes this kind of HPP topology as more matured and readily deployable.

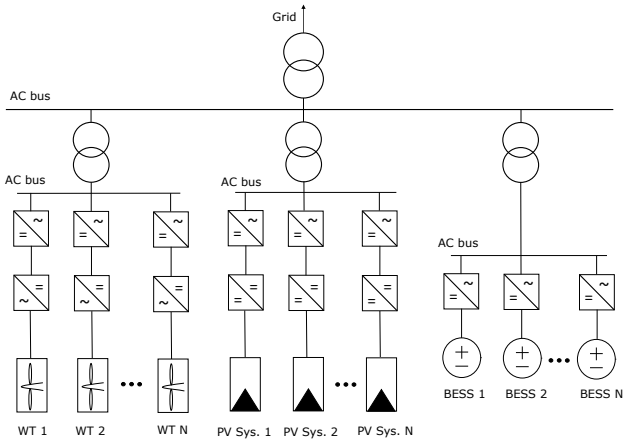

Fig. 1. Topology of an AC connected HPP

As depicted in Fig. 2, a DC-coupled HPP is comprised of multiple DC-coupled hybrid units. Each hybrid unit consists of a WT, a PV system, and a BESS. In this topology, the various assets are connected together at the DC-link forming an hybrid unit, which is further connected together with the other hybrid units through an inverter at the AC substation, which interfaces the hybrid units to the external grid. The WT's connection to the DC bus requires a rectifier, whereas the PVs and the BESSs are connected via DC-DC converters. It is worth noticing that the different control schemes at asset level need to be integrated to communicate with the plant controller. The primary benefit that arises from this HPP topology is the capital expenditure reduction, due to using fewer components for electricity conversion. In particular, the DC to AC conversion is handled by a single inverter, in contrast with the AC-coupled HPP topology, that requires three DC/AC converters [2]. However, major challenge arises from development of new controllers for controlling Hybrid units.

III. Hybrid Power plant Control Architecture

The overall HPP control architecture for both AC- and DC- coupled topologies is depicted in Fig. 3. It consists of the HPP control level (central control level) and the unit/asset control level (local control level). Notice that in the case of AC-coupled HPP topology, the local control level corresponds to the individual asset control level, namely WT, PV and BESS control level, while in the case of DC-coupled HPP topology, the local control level corresponds to hybrid unit control level. Each unit/asset exchanges signals with the HPP control level, which in turn, communicates with the system operators as well.

The main goal of the HPP control level is to control the active power exchange between the HPP and the grid centrally. The HPP control level acts as a single central unit,

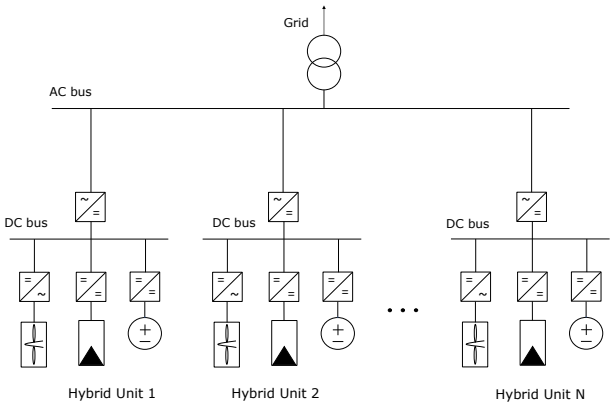

Fig. 2. Topology of a DC connected HPP

controlling the power production of the HPP by sending out power references to the unit/asset control level. These power references are generated based on both measurements in the point of common coupling (PCC) and the available power of each individual unit/asset. The total available active power can be defined as the optimal active power production from the WTs and solar PV plant according to the input weather conditions, i.e. wind speed and solar irradiation. The local control level ensures that the power reference signals derived by the HPP central control level are achieved.

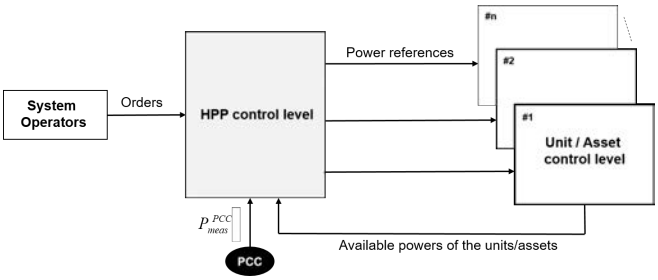

Fig. 3. Hybrid power plant control level structure.

The system operators order the production of the HPP, i.e. either maximum production or production regulation according to various control tasks. Also, they supervise the behaviour of the HPP and depending on the actual network status, they issue specific demands to the HPP central control level.

The HPP control level, depicted in more details in Fig. 4, has as task to control the HPP power production to the reference power ordered by the system operator. It contains a control functions block, the HPP controller itself and a dispatch function block. Each block has a specific role in transmitting the power orders, given by the system operators, into power references that are sent throughout the entire HPP. At the present stage, the signal communication between the HPP control level and the units/assets is neglected.

The given orders by the system operators can be executed [7] according to one of the control functions visualised in Fig. 5, namely:

- *Maximum power production*, where the HPP is required to generate power equal to the available power, depending the weather conditions.

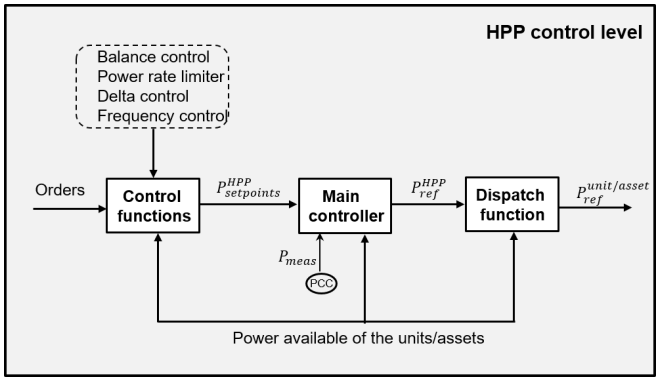

Fig. 4. Hybrid power plant control system configuration.

- *Balance control*, where the HPP production can be adjusted downwards or upwards in steps at constant levels.
- *Delta control*, where the HPP operates with a reserve capacity in relation to its momentary possible power production capacity.
- *Power gradient limiter*, that sets how fast the total active power production can be adjusted both upwards and downwards.

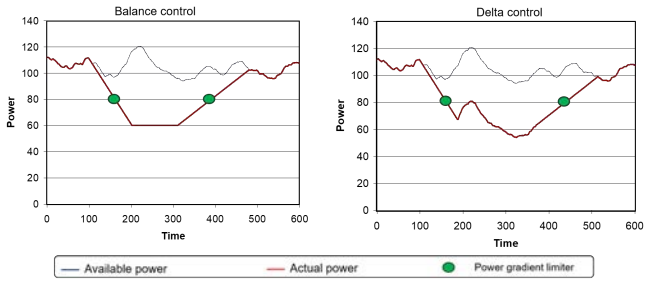

Fig. 5. Control functions

Notice that all these control functions can be implemented in such a way that they can be enabled at the same time.

The aim of the HPP main controller is to ensure that the HPP power setpoints, generated by the control function block, are achieved. An extension of the HPP main controller with a frequency controller, as described in [8], can be performed with the task to detect any possible frequency deviation from its rated value (50Hz) and translate it into an active power signal. The output of the main controller is the HPP power reference, which is further used by the dispatch function block, which further distributes the power references to the individual units/assets.

IV. Hybrid power plant dynamic modelling

In this section the developed HPP dynamic model, consisting of sub-models for Permanent Magnet Synchronous Generator (PMSG) wind turbine, solar PV, and BESS are shortly described.

A. Wind turbine model

The implemented wind turbine model is described in details in [9].

A typical configuration of a variable speed wind turbine based on a multi-pole permanent magnet synchronous generator (PMSG) is illustrated Fig. 6. In this configuration, the PMSG synchronous generator is connected to the grid through a full-scale frequency converter system that controls the speed of the generator and the power flow to the grid. The full-scale frequency converter system consists of a back-to-back converter, i.e. generator-side converter (rectifier) and the grid-side converter (inverter) connected through a DC link. As illustrated in Fig. 6, the aerodynamic rotor of the wind turbine is directly coupled to the generator without any gearbox, i.e. through a gearless drive train. Since the generator is connected to the grid through the frequency converters, its electric frequency is fully decoupled from the frequency of the power system. This allows for variation in the generators electrical frequency according to the wind speed changes, while the network frequency remains unaffected. Therefore, the frequency on the generator side can be controlled either to match the optimized mechanical frequency of the aerodynamic rotor or to deviate from it whenever desired.

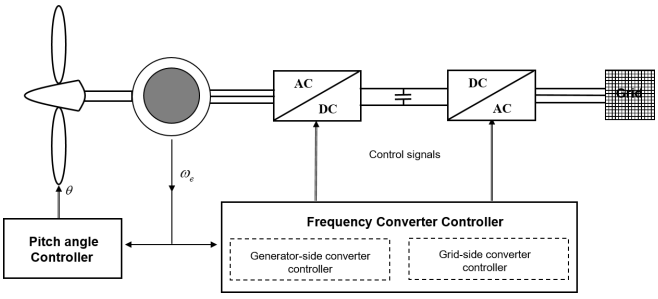

Fig. 6. Variable speed multi-pole PMSG wind turbine configuration.

The control system of such WT consists thus of two controllers: the pitch angle controller and the frequency converter controller. Both controllers are using information about the generator speed. The WT's power production and the generator speed are controlled by the frequency converter according to an optimal power characteristic, most commonly known as Maximum Power Point Tracking (MPPT). The pitch angle controller controls the generator speed by pitching the WT's blades, being operationally active only at high wind speeds.

B. Solar PV model

The overall solar PV block model, based on the generic WECC model for large-scale PV plants described in details in [10] and [11], is illustrated in Fig. 7. The PV system receives as external inputs the weather conditions, as a set of solar radiation (E) and temperature (T), which together define the available solar power at any moment. Additionally, the voltage on both the PV terminal and the DC-link are measured. The former is essential for the MPPT implementation, whereas the latter is used to calculate the alpha ratio of the DC-DC converter. The PV system control block specifies the output current of the PV, which along with the voltage on the PV terminal, make up the power output of the PV system. The PV module block incorporates the Maximum Power Point tracking (MPPT), where according to both the PV

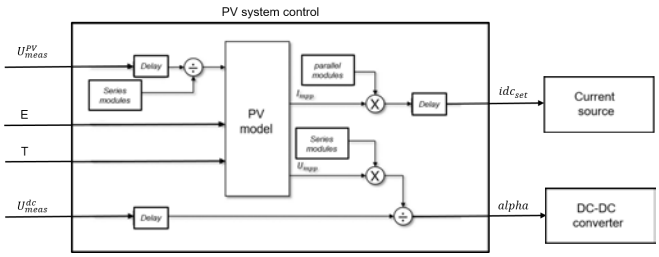

Fig. 7. Solar PV model structure.

voltage and the weather conditions the optimal output current and voltage are specified. The former is the input to the current source, while the latter is used to define alpha, after dividing it with the DC-link voltage. Measurement delays both on voltage inputs and on input signal to the current source are incorporated in the model.

C. Battery Energy Storage System model

The Battery Energy Storage System (BESS) model, consisting of models for the battery, the systems's PQ and charge control, are described in details in [4] and [5]. The BESS control block diagram is depicted in Fig. 8. Depending on both the input reference signal and the storage availability, expressed by the state of charge (SOC), the charge control block defines whether the battery needs to be charged, discharged or stay inactive. The voltage set-point specification block then receives the current reference signal from the charge controller, as well as the battery terminal voltage from the battery block, generating the voltage source set-point value. The battery block diagram, depicted in Fig. 9,

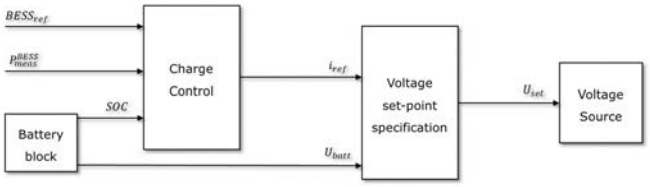

Fig. 8. BESS control block diagram

models the battery itself while also specifies the alpha value. It should be noted that the internal voltage of the battery varies depending on the SOC. As presented in [5], alpha

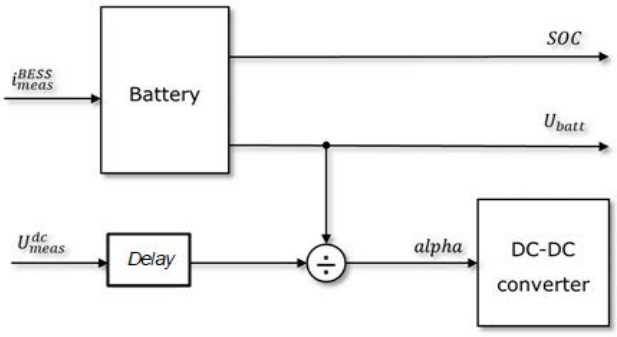

Fig. 9. Battery block diagram

is calculated by the DC terminal and the battery terminal voltages similarly as in the PV system. The battery model gets the BESS current as input and depending solely on that it updates its SOC. The charge control block consists of a PI controller defining the output reference value after comparing the reference signal to the active power measurement. Additionally, a charge limiter can be interposed to prevent the battery from charging or discharging if it is full or empty, respectively.

D. Ancillary services

Dynamic modelling for ancillary service provision from HPP also depends on HPP topology and control architecture. Frequency control can be implemented at HPP control level in conjunction with other control levels invariant with topology. However, low voltage ride through (LVRT) support depends completely on the topology. LVRT support from AC coupled HPP is same as that of traditional WPP. However, additional challenges lie in developing the control for LVRT in DC coupled HPP, since PV and storage are also connected at the DC bus of the WT.

1) Frequency Control: Droop and derivative based frequency control, shown in Fig. 10, is described in details in [8].

Both droop and derivative act in similar way: when the frequency and rate of change of frequency is beyond the deadband, constant gain is applied. The output of the controller, DP is the additional power output order to provide frequency support. In order to provide, frequency containment reserve, either the reserve should be available in the battery storage or the wind/PV needs to be operating in curtailed operation before the disturbance. Where as, fast frequency response can be provided either by battery storage or by extracting the kinetic energy from the rotor of the WTs.

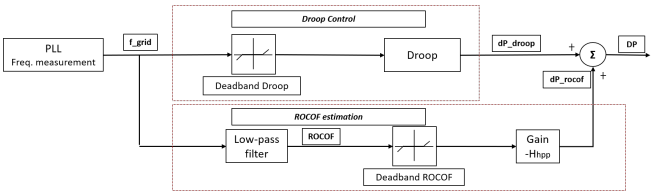

Fig. 10. Block diagram of the frequency controller

2) Low Voltage Ride Through: Fig. 11 depicts the LVRT control for DC coupled HPP . The dq current references I_{dref} and I_{qref} are sent to the Grid-side converter of the DC coupled HPP, shown in Fig. 2. According to this control, the reference reactive current Q_{ref} is the outcome of the error between the reference grid voltage $U_{grid,ref}$ and the measured grid voltage $U_{grid,meas}$. As explained in [12], the error is regulated by a PI controller and defines how much reactive current is required during the fault.

Correspondingly, the difference between the reference DC-link voltage $U_{dc,ref}$ and the measured voltage at the DC-link $U_{dc,meas}$, produces the d-axis component of the grid-side converter current (I_d), through another PI controller. It should be notice that the grid-side converter dq-axis current capacity is limited through a current limiter. Whenever the main aim is to provide LVRT support to the grid, while

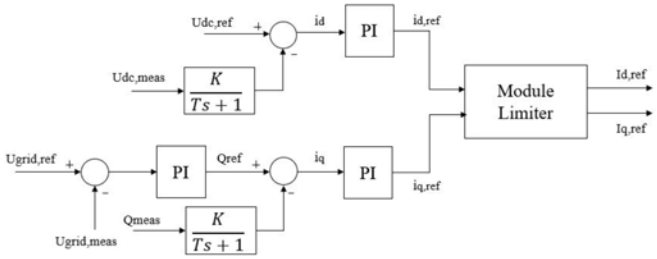

Fig. 11. AC voltage control of grid side converter for LVRT support in a DC coupled HPP [12]

the frequency support is a secondary service, the q-axis component is prioritized.

V. Performance Results

In order to investigate the performance of the presented HPP model and control a set of simulations are carried out using an HPP comprising of 60 X 2 MW Type 4 WTs, 40 MW of PV and 10 MW/20MWh Battery storage. Fig. 12 shows the dispatch of wind power, solar power and battery storage for different control functions. In these studies, wind speed is assumed to be varying between $11.4-11.9m/s$ and solar irradiance varies between $980-1000W/m^2$. Battery SOC is assumed 0.8pu.

In Zone A, the HPP operates in maximum power point tracking mode (MPPT), where all the generators generate as per maximum available power. It should be noted that the BESS neither charges or discharges at this point. In Zone B, a delta control mode is imposed, namely a reduction of the HPP power by 10 MW is received by the HPP controller. This 10 MW can be considered as reserve for handling contingencies. Notice that in order to meet this power curtailment, BESS is charged to its maximum capacity of 10MW. If the power reduction requirement is more than the power capacity of the BESS, the power need to be curtailed by either WTs or PV plant. This is the case in Zone C. The HPP is now ordered into the balanced control mode at 65 MW. This is achieved by curtailing the wind power. The ramp rate limitations of 7 MW/s has been applied for the HPP which can be seen from the fact that wind power output reduces from 110 MW at 80s to 40 MW at 90s. It should be noticed that in this investigation during curtailment, WT is prioritised for curtailment instead for PV . However, this decision should be taken in practice based on lifetime and cost analysis. Similarly, the battery charging and discharging strategy is quite simple in these studies. Practically, BESS dispatch strategy can be based on market based optimisation. In Zone D, the HPP is again to operate in MPPT control mode and WTs, PV produce available power. Consequently, BESS is recharged, namely stops consuming charging current and produces/consumes 0 MW.

Figure 13 depicts the HPP active power output, the frequency at the PCC, as well as the output of the droop and derivative control for a DC coupled HPP - with and without frequency controller. In the first 40 seconds, the power output remains at 120 MW, following the ordered amount of reserve capacity. When the frequency change is observed, the power output of the HPP increases to support the frequency. This increase is not instantaneous as a result of

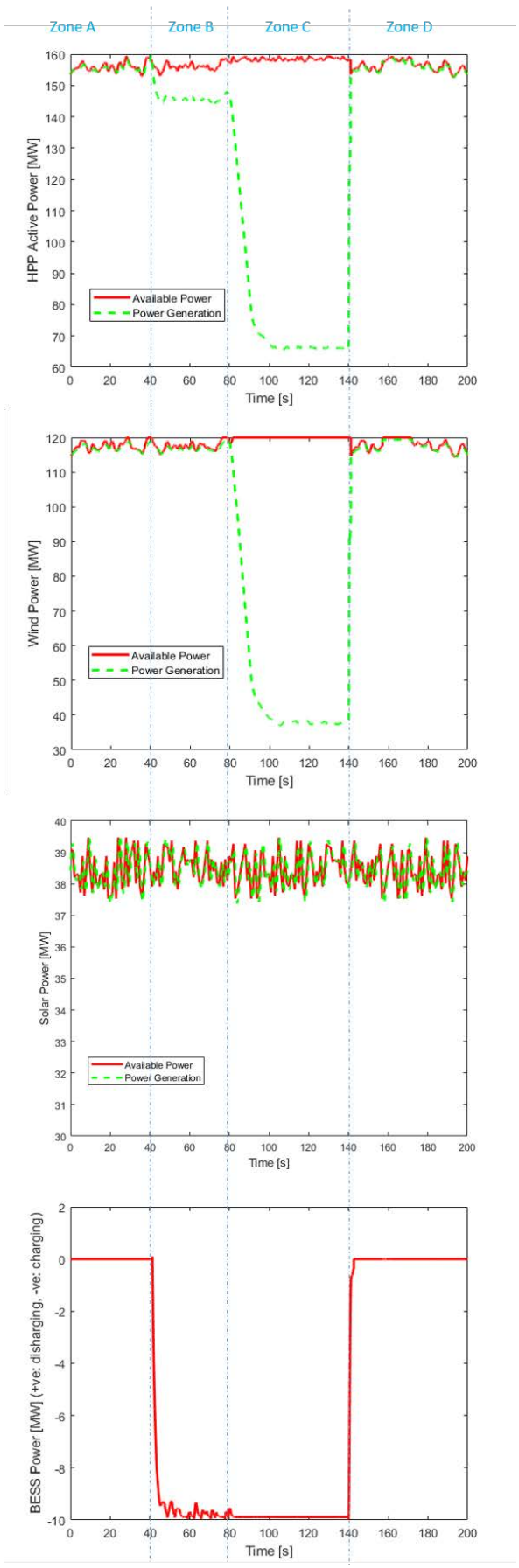

Fig. 12. Active power response of the HPP and assets at the PCC under different control function commands and changing weather conditions

both the frequency measurement and communication delays (as the frequency control is implemented at HPP controller level). Frequency event is created based on power system model and event in [13]. It is evident that the frequency control improves the nadir to 49.536 Hz. The bottom graph shows the output of the frequency controller. Given the increased ROCOF during the first moments, the derivative control is activated initially. When the frequency reaches the nadir point though,derivative action is made zero as a result of an additional constraint. This is due to the fact that without this constraint the derivative loop would take negative values, counteracting thus the effect that the droop control has. The droop control remains active throughout the event, resulting in the power output as seen in the Fig. 13.

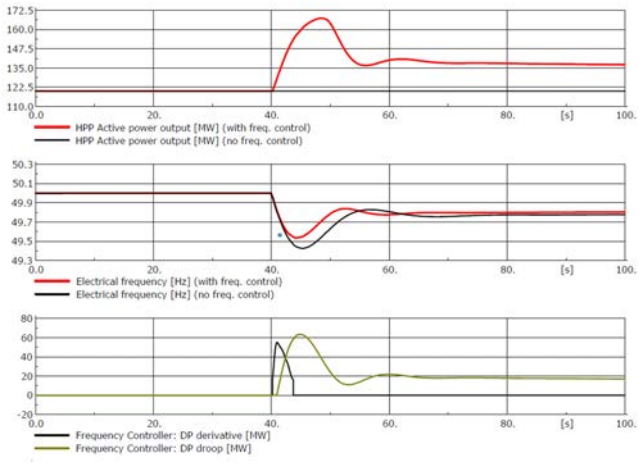

Fig. 13. HPP output and frequency controller response during a frequency event - with and without frequency controller

Figure 14 illustrates the power output of the individual assets. It should be noticed that only the BESS and the WT participate in the frequency support action. The former changes its state from charging to discharging to cover the demand for increased power production. At $t = 50s$ though, it stops contributing as the WT takes over. This decision can be made based on multiple constraints and logics - such as - battery size, the reserve available in the WT, optimization/dispatch strategy.

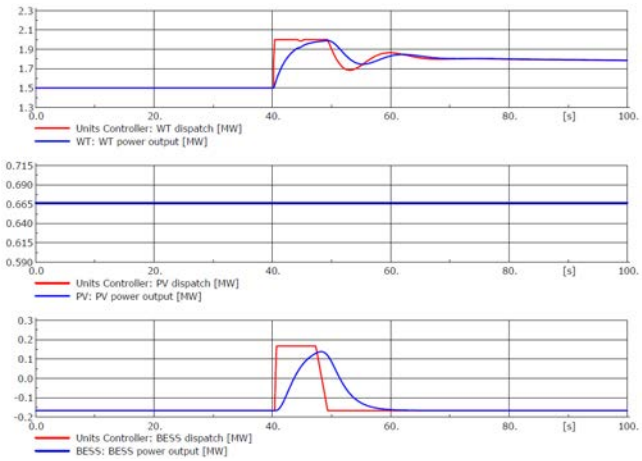

Fig. 14. Output of HPP assets during a frequency event

VI. Conclusion

This paper provides an overview of different HPP topologies and dynamic models for the assets of wind-PV-storage based HPP. The performances and challenges of dynamic models are demonstrated through simulations.

Acknowledgment

This work is done as part of Indo-Danish project "HYBRIDize" funded by Danish Innovationsfonden (IFD)

References

[1] K. Das *et al.*, "Enhanced features of wind based hybrid power plants," in *Proceedings of the 4th International Hybrid Power Systems Workshop, Crete, Greece*, 2019.

[2] L. Petersen *et al.*, "Vestas power plant solutions integrating wind, solar pv and energy storage," in *Proceedings of the 3rd International Hybrid Power Systems Workshop, Tenerife, Spain*, 2018.

[3] WindEurope, "Renewable hybrid power plants," https://windeurope.org/wp-content/uploads/files/policy/position-papers/WindEurope-renewable-hybrid-power-plants-benefits-and-market-opportunities.pdf, July 2019, accessed on 07 Oct 2019.

[4] P. Adamou, "Dynamic hybrid park simulation for co-located hpp for frequency ancillary services," MSc Thesis, DTU Wind Energy, 2019.

[5] X. Giagkou, "Dynamic modelling and control of dc-coupled hpp for frequency support," MSc Thesis, DTU Wind Energy, 2019.

[6] S. Afxentis *et al.*, "Promotion of higher penetration of distributed pv through for all (stores)," in *INCREaSE: Proceedings of the 1st International Congress on Engineering and Sustainabilty in the XXI Century*. Springer, 2017.

[7] A. D. Hansen, P. Sørensen, F. Iov, and F. Blaabjerg, "Centralised power control of wind farm with doubly fed induction generators," *Renewable energy*, vol. 31, no. 7, pp. 935–951, 2006.

[8] D. V. Pombo, F. Iov, and D. Stroe, "A novel control architecture for hybrid power plants to provide coordinated frequency reserves," MSc Thesis, Aalborg University, 2019.

[9] A. D. Hansen, F. Iov, P. E. Sørensen, N. A. Cutululis, C. Jauch, and F. Blaabjerg, "Dynamic wind turbine models in power system simulation tool digsilent," 2007.

[10] J. Ma, D.-W. Zhao, M.-H. Qian, L.-Z. Zhu, and H. Geng, "Modelling and validating photovoltaic power inverter model for power system stability analysis," *The Journal of Engineering*, vol. 2017, no. 13, pp. 1605–1609, 2017.

[11] C. I. Ciontea, D. Sera, and F. Iov, "Influence of resolution of the input data on distributed generation integration studies," in *2014 International Conference on Optimization of Electrical and Electronic Equipment (OPTIM)*. IEEE, 2014, pp. 673–680.

[12] n. . M. Filipos Rigas, title = Voltage support form Hybrid Power Plants.

[13] A. Adamczyk, M. Altin, Ö. Göksu, R. Teodorescu, and F. Iov, "Generic 12-bus test system for wind power integration studies," in *2013 15th European Conference on Power Electronics and Applications (EPE)*. IEEE, 2013, pp. 1–6.